J. Reprod. Fert. (1984) **70**, 511–523 *Printed in Great Britain*

Observations on the response of human spermatozoa to gravity, boundaries and fluid shear

H. Winet, G. S. Bernstein and J. Head

Department of Obstetrics and Gynecology, University of Southern California School of Medicine, Los Angeles, CA 90033, U.S.A.

Summary. Human sperm motility response to three mechanical stimuli, gravity, fluid flow shear and rigid boundaries, was measured in a tube of 310 × 400 μm calibre. Data were gathered by cine recordings at various focussing levels d across the tube and analysed with a computerized image analysis system. The most influential stimulus was the tube wall near (more than 'at') which the swimmers tended to accumulate, leaving the fluid beyond 100 μm from the wall (d = 100) vacant of motile spermatozoa. The boundary effect was evident as soon as the spermatozoa could be viewed after loading, and accumulation, measured as frequency, as a function of d did not change with time *t*. This response was not significantly altered by the addition of laminar flow with a centre line velocity of about 400 μm/sec. In flow shear, spermatozoa aligned positively (in the flow direction) at the wall but negatively by about 30 μm from the wall where the velocity gradient (= shear rate) was about 3·5 sec^{-1}. The response to gravity was relatively weak with 11 spermatozoa positive (swimming downwards) for each 9 negative. Neither the boundary effect nor the 'rheotaxic' effect were influenced by gravity as there was no statistical difference in orientation or distribution patterns between vertically and horizontally flowing suspensions.

It is suggested that the boundary effect cannot be ignored in in-vitro manipulations, particularly when spermatozoa are observed or extracted. Its importance *in vivo* lies in the degree to which the tubes transporting motile spermatozoa seem to have mechanisms for reversing the wall accumulation tendency.

Introduction

There is no evidence that spermatozoa have physiological transduction systems for processing mechanical information from their environment. They have been shown, however, to respond to differences in flowing fluid velocity from one side (or end) of their body to the other (Adolphi, 1905; Bretherton & Rothschild, 1961; Roberts, 1970; but see Kono, Morohashi, Kinose, Hiura & Yamamoto, 1977, for conflicting results) and to accumulate at liquid-wall interfaces (Rothschild, 1963) as well as beat in synchrony when closely packed (Walton, 1952). In addition they have been supposed to prefer swimming downwards in a uniform density fluid (Roberts, 1972; Katz & Pedrotti, 1977). These apparent taxes, 'rheotaxis', 'thigmotaxis' and 'geotaxis', respectively, have all been studied separately. Two have become bases for explaining apparent success in techniques for separating X- and Y-chromosome bearing spermatozoa (Ericsson, Langevin & Nishino, 1973; Bhattacharya, Shome & Gunther, 1977; Sarkar, 1981). Only Roberts (1970) has investigated the interaction of stimuli (flow and gravity) but he used 200–300 μm bore tubes which were observed in horizontal orientation only so there was little room for the 50 μm long bull spermatozoa used to develop a geotaxic response.

0022-4251/84/020511-13$02·00/0

Gravity is assumed to be critical in clinical manipulations *in vitro* such as the X–Y separation technique of Ericsson *et al.* (1973). Fluid flow is encountered often by spermatozoa *in vivo* and orientation in flow has been utilized for motility assessment (Atherton, 1975). Moreover, no container is unbounded so spermatozoa must interact with vessel walls. The apparent random investigation of these mechanotaxes indicated to us a need to determine the relative importance of each of them interacting in a 'real' system with known boundary conditions. Definitive results from such an investigation would allow one to estimate where motile spermatozoa tend to accumulate in a specified system. The present report provides quantitative evaluation of human spermatozoa responding simultaneously to gravity, fluid flow and the proximity of boundaries.

Materials and Methods

Semen was obtained by masturbation from normal male participants in the fertility clinic run by G.S.B. The samples were chosen for maximum motility and concentration by an experienced semen analysis technician. All observations were performed 1–5 h after collection and were carried out in a room maintained at 30–32°C. Each semen sample was diluted 20 : 1 with RPMI$^+$ medium which consisted of RPMI (Rose Park Military Institute medium, an amino acid-enriched cell culture medium) 1640 (Irvine Scientific, Irvine, CA) fortified with 0·03% glutamine, 0·1% fructose and 0·5% fetal calf serum (after S. Sarkar, personal communication). This sperm suspension was drawn through polyethylene tubing into a 20 ml syringe which was rocked before mounting to ensure mixing of the cells. The syringe was then mounted in an infusion pump (Harvard No. 901) and pumped immediately through about 50 cm of polyethylene cylindrical tubing to a 'rectangular' capillary tube (Vitro Dynamics, Rockaway, NJ) which was 50 mm long and 310 × 4000 μm in lumen dimensions. All glassware was siliconized to prevent electrostatic adherence of the cells to the chamber walls.

The behaviour of the spermatozoa in the chamber was observed by means of the system shown in Text-fig. 1. A pin-registered 16 mm cine camera (Photo Sonics, No. P/N 61-1000) loaded with Kodak 2475 instrumentation film was used for recording. Observations consisted of focussing on successive vertical optical planes across the chamber with the microscope fine adjustment. At each plane we took a 3-sec film-burst at 16 frames/sec (sufficient to follow the sperm path arc) and the sequence identity was simultaneously recorded on audio tape. Magnification was sufficient to observe sperm tails of immotile cells but scale calibration was ensured by photographing a stage

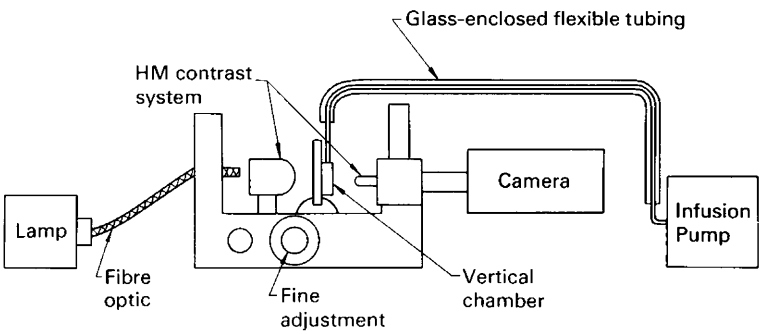

Text-fig. 1. The general set-up for observing sperm 'mechanotaxes'. The sperm suspensions were pumped from a syringe mounted in the infusion pump via flexible tubing to or through the vertical or horizontal chamber and on via more flexible tubing to an open beaker. The glass tubing surrounding the flexible tubing eliminated vibrations that would create pressure waves in the suspensions. A × 10 Hoffman Modulation (HM) contrast objective received the image field and transmitted it to the camera through the microscope. The HM contrast condenser was fitted with an infrared filter and was illuminated with a fibre optic–halogen lamp system.

micrometer. The chamber was mounted on a polarizing microscope stage which was calibrated in degrees so it could be rotated exactly 90° for lateral or vertical reorientation.

Geotaxis was observed in chambers oriented vertically. It was quantitatively represented as a frequency, with the geotaxis ratio G_r the reference quantity. This ratio is defined as

$$G_r = \frac{\text{population of spermatozoa swimming upwards}}{\text{population of spermatozoa swimming downwards}}$$

Rheotaxis was observed in vertically or horizontally orientated chambers with flow upwards or lateral respectively. In preliminary studies (Winet & Head, 1982) we found no difference between upward and downward results so we reduced vertical observations to upwards only. In all cases the optical plane was parallel with the two longest axes of the chamber as indicated in Text-fig. 2. This setup did not allow assessment of any component of motion at an angle to the optical plane. But error from this limitation was minimized by restricting analysis to only those spermatozoa that remained in the plane of focus for at least 0·625 sec and were swimming at at least 30 μm/sec, i.e. covered 18 μm. The depth of field for the microscope objective used was 4 μm. Consequently, only those spermatozoa whose swimming paths were $\leq 12{\cdot}5°$ to the ideal swimming path (which would be in the plane perpendicular to the optical axis, see Text-fig. 2) were included in the analysis.

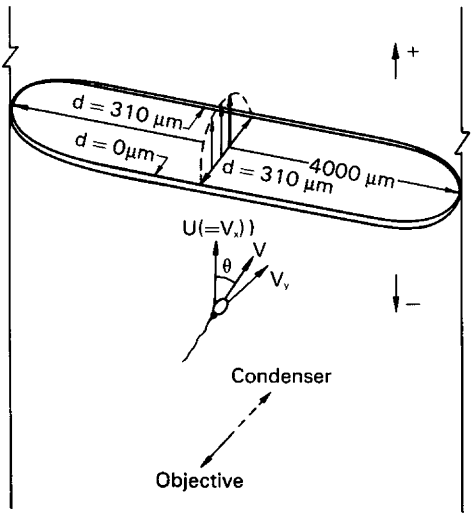

Text-fig. 2. Definition of measured quantities and dimensions of the chamber section which served as the observation tube. The observation field was equidistant from the chamber ends. D is the shortest inner dimension of the tube which crosses the tube long axis; d is any point along the D line; u(d) is a function describing the fluid velocity parallel to the tube axis for each d value and therefore defines a flow velocity profile which has been drawn in the figure. Any velocity component in the same direction as u(d) is positive. V is the resultant velocity of a spermatozoon, U ($= V_x$) the component of V in the u(d) direction and θ the angle between U and V. V_y is the component of V in the direction of d. The third component V_z in the direction of the long width of the tube is not shown but would have to be included in the true value of θ which is generally not confined to a plane parallel to any of the 3 co-ordinate planes. The arrows showing the direction of the objective and condenser also parallel D and the optical axis.

Fluid flow was detected by the addition of 1 μm polystyrene latex spheres to the suspension and constructing a flow velocity profile from analysis of films of the motion of these tracers. No velocity difference was detected between immotile spermatozoa and tracers located the same distance from the wall. The swimming components in the direction of fluid flow were designated positive and those in the opposite direction negative. Accordingly, the true swimming velocity in flow

experiments was obtained by subtracting the profile velocity value at the appropriate depth, u(d) (see Text-fig. 2), from the swimming component parallel with the flow axis, U. A quantitative measure of rheotaxis could then be obtained as the degree to which the spermatozoa lined up with u(d) at each d or velocity gradient (the slope of the flow profile at d). The measure we chose was the cosine of the angle θ between u(d) and the resultant velocity V of the observed spermatozoon (Text-fig. 2). Therefore, maximum positive rheotaxis would have the value 1·00 and maximum negative rheotaxis the value −1·00.

The third quantity analysed was the interaction or "inelastic collisions" (Rothschild, 1963) of spermatozoa with the chamber walls. These were evaluated as frequency distributions, an obvious continuation of the appropriate model from kinetic theory. We did not, however, go so far as to assume spermatozoa were molecules and would follow Boltzman distribution patterns. Instead we compared observations statistically by obtaining a purely empirical polynomial regression line for each reference set of data and applying the F statistic procedure for goodness-of-fit of other sets to this curve as described by Pollard (1977). Therefore the only curves in this study that have physical meaning (i.e. are representative of physical laws) are the flow velocity profiles. All the others are strictly empirical. Rothschild (1963) was emphasizing this empiricism when he put quotes around "inelastic collisions" to describe the 'thigmotactic' effect. Accordingly, we would learn no more about the mechanism for sperm distribution by merely increasing the degree of a regression polynomial until finding the 'best fit' than we would by employing curves which are: (a) as small in degree as possible yet still able to achieve a $Q \leq 0{\cdot}001$ level of confidence (this value is equivalent to a P level in Student's t test of better than 99·9% confidence) in accordance with the Principle of Parsimony and (2) the best fit for the degree used. Accordingly, we may expect regression lines that do not follow all the points in a scatter diagram or that exceed 'realistic' value limits, because the only question addressed by this statistical tool is: "Is there any statistically significant difference between how well a regression line fits the data for population A and how well it fits those for population B when it has already fit one of the two populations to a high level of confidence?"

A NAC (Instrumentation Marketing, Burbank, CA)-plus-HP-85 ciné analysis system was used to digitize the frame number and x–y co-ordinates of the moving sperm midpiece or tracer particle. Only cells swimming a relatively straight line for at least 10 frames were utilized. This information was transmitted to the computer which stored the data on tape and processed them for computations.

Results

Results of observations of 5 samples for geotaxic behaviour are presented in Table 1. The average G_r for all samples was $0{\cdot}819 \pm 0{\cdot}222$, i.e. 55% of the spermatozoa were positively geotaxic and swam downwards. The positive geotaxis tendency was expected from the predictions of Roberts (1972) and Katz & Pedrotti (1977). The smallness of this tendency was not, however, addressed by these studies.

According to the predictions of Roberts (1970) the geotaxic response of spermatozoa interacts with rheotaxis to produce a non-symmetrical orientation pattern across the tube during lateral flow.

Table 1. Geotaxis ratio in each of 5 sperm samples as a function of time after tube loading

	Geotaxis ratio G_r				
Min	Sample 1	Sample 2	Sample 3	Sample 4	Sample 5
0	0·642	0·848	0·800	0·606	—
30	0·727	1·188	0·500	0·934	1·000
45	0·615	0·745	0·906	0·508	0·903
60	1·286	1·000	—	0·927	0·606

Thus, the cosine of the angle θ (see Text-fig. 2) formed by the resultant swimming velocity of each sperm V and the flow velocity, u(d), will be predominately '+' in the upper and '−' in the lower half of the horizontal tube. We are assuming, of course, positive rheotaxis for spermatozoa moving towards the tube axis (in the upper half of the tube) and negative rheotaxis for those moving towards the wall. In the present setup we were focussing horizontally, not vertically as did Roberts (1970). There is therefore no reason to expect any gravity-related difference in the distribution or orientation of spermatozoa between the 'near' and 'far' halves of the tube. This expectation is borne out by the axisymmetry of the LAT scatter diagram regression line of Text-fig. 3. However, gravity-related differences between UP and LAT orientation regression curves are expected if geotaxis is of sufficient magnitude in comparison with rheotaxis. Such an expectation is based upon simple summation of the predicted rheotaxic and geotaxic swimming directions; being parallel in UP systems and perpendicular in LAT systems. Cos θ would then tend towards ± 1·00 in vertical tubes where geotaxis is in the direction of rheotaxis and 0·00 if opposite in sense. Roberts (1970) predicted a negative rheotaxis and positive geotaxis for spermatozoa so one would expect a cos θ tending to − 1·00 at the d where rheotaxis is optimal in UP tubes. In contrast, a strong enough geotaxis will reduce any rheotaxic effect in LAT tubes because the two factors are perpendicular. Given these conditions we would predict that LAT and UP scatter diagrams (Text-figs 3 & 4) would be statistically distinguishable. The polynomial plots shown are the lowest degree regression lines which fit their respective scatter diagrams to an F statistic goodness-of-fit confidence level of $Q < 0{\cdot}001$. In Text-fig. 3 the curves are of second degree.

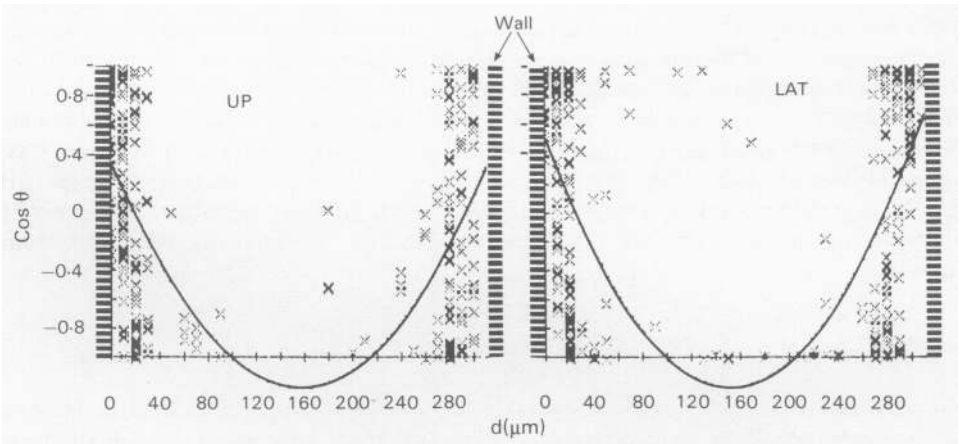

Text-fig. 3. A scatter diagram of individual sperm cos θ's as functions of d. Raw data along the entire D are shown. Each datum point (x) represents a single spermatozoon and is shown as generated by the computer printer because hand drawings would be unfeasible. Point density is therefore an indicator of frequency.

The scatter diagram comparison procedure consists of applying the F statistic test to evaluate the goodness-of-fit of the UP curve to the LAT data (or *vice versa*). Again we obtain a confidence level of $Q < 0{\cdot}001$. This result means that there is no statistical difference between the UP and LAT scatter diagrams for the entire d = 0 to d = 310 μm chamber cross-section.

The overshoot of the *x*-axis by these regression curves is a direct reflection of the high concentration of spermatozoa near the walls. While this effect does not invalidate our application of the F statistic, it produces 'unrealistic'-looking curves unless we select at least 4th degree polynomials. We can enhance curve fit by taking advantage of the axisymmetry of the data and lumping the mirror images together before computing the regression curve.

Thus, data from $0 \leq d \leq 155$ μm are considered a mirror image of those from $155 \leq d \leq 310$ μm and the values are combined and averaged in Text-fig. 4 before computing a least squares polynomial fit. A third degree polynomial was chosen to improve goodness-of-fit and reduce axis overshoot. Note the change in sign of $\cos\theta$ in the region $20 \leq d \leq 30$ μm and the high positive value of $\cos\theta$ at the wall in both plots.

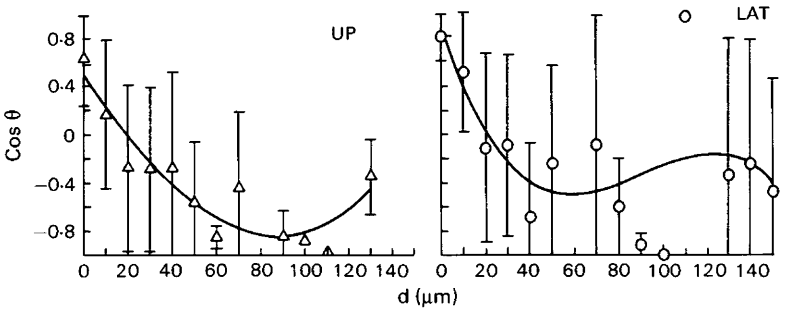

Text-fig. 4. The same data that yielded Text-fig. 3 combined and averaged according to the mirror image assumption of sperm behaviour along the D axis. Error bars are s.d.

The swimming velocity component U parallel to the flow axis is plotted as a function of d in Text-fig. 5. The U values came from the same spermatozoa as did the $\cos\theta$ values. The two regression curves (third degree polynomials) fit their own datum points at the $Q < 0{\cdot}001$ confidence level. Moreover, the UP scatter diagram regression curve fits the LAT scatter diagram at $Q < 0{\cdot}001$. Therefore, the distribution of U as a function of d shows the same lack of UP *versus* LAT discrimination as does the $\cos\theta$ data.

The dimensions of the ordinate allow us to include the flow velocity profile in Text-fig. 5. As a consequence we can relate any changes in U to changes in flow velocity, i.e. the velocity gradient at the d (actually small segment of D) where the changes occur. Thus U is positive at the wall but changes sign in the region $40 \leq d \leq 60$ μm. In this segment of the flow profile the velocity gradient is 3·46 (UP) to 3·76 (LAT) sec^{-1}.

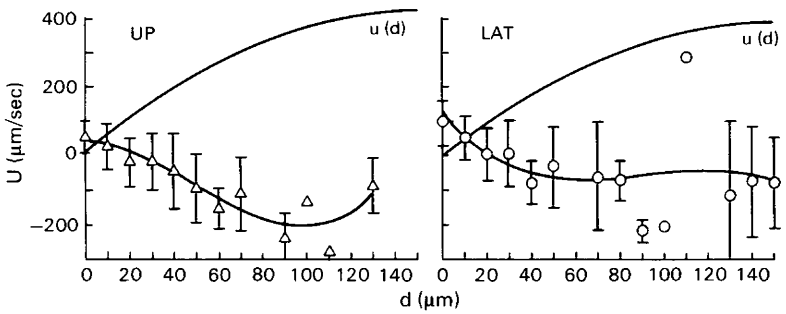

Text-fig. 5. The average U velocity components as functions of d for the same spermatozoa yielding Text-figs 3 and 4. The upper curve is the average flow velocity profile for the 5 semen samples. The maximum fluid velocity is about 400 μm/sec which yields a volumetric flow rate of $\sim 2{\cdot}5 \times 10^{-4}$ ml/sec for the chamber.

The final quantity measured was frequency distribution of spermatozoa as a function of d (Text-figs 6–8). The spermatozoa represented in Text-fig. 6 are those providing data in the previous figures. The sperm suspension was mixed just before it was pumped into the observation tube and the data so far described were obtained from observations made about 30 min after this initial

pumping at $t = 0$ min. In Text-figs 7 and 8, showing frequency distributions as functions of t, the specimens utilized for this evaluation were the same as those used for the geotaxis study. Again, a third degree regression polynomial is utilized to characterize the relationship of f to d.

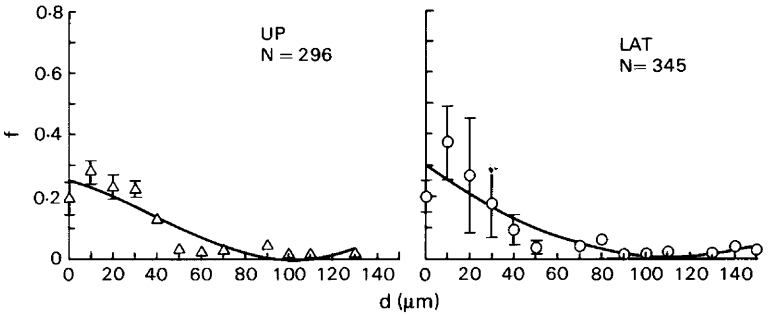

Text-fig. 6. Frequency distribution of spermatozoa as a function of d for the same cells yielding Text-figs 3–5. N = total number of spermatozoa. Frequency averages do not total 1·00 in this and each of the following text-figures because they do not all represent 5 semen samples. Values with error bars represent 2–5 samples. From 1 to 5 samples are represented by each f = 0 value because some error bars merge with the x-axis.

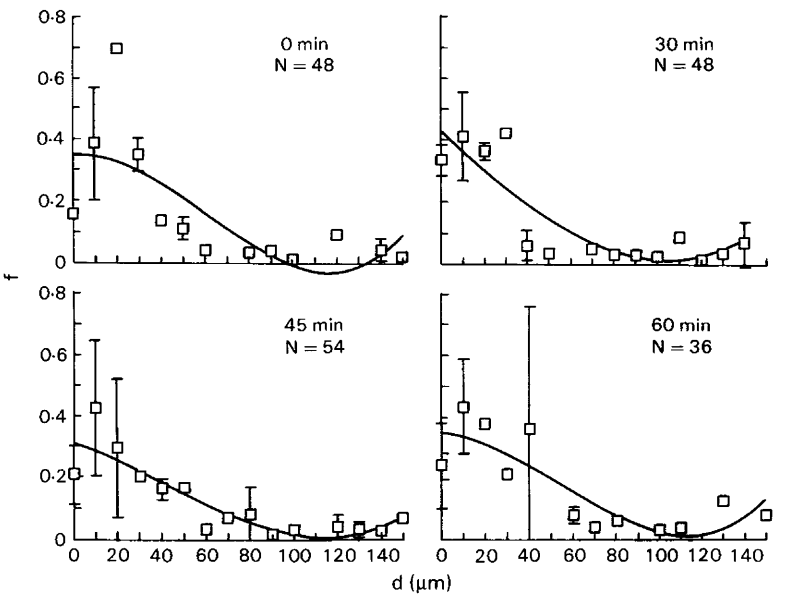

Text-fig. 7. Frequency distribution of spermatozoa as a function of d for different times after pumping of the first spermatozoa of a sample into the chamber. The fluid here is static. N = total number of frequencies used.

A statistical matching of each distribution with that at $t = 0$ is presented in Table 2. Data are the same as those yielding the plots in Text-fig. 7. The degrees of freedom or ν_1 and ν_2 where ν_1 = number of distinct d values − number of regression curve coefficients and ν_2 = number of datum points − number of distinct d values, are used to find Q in F-distribution tables. Q is a function of F, the variance-ratio, where F = lack-of-fit mean squares ÷ pure error mean square. A large F value means that variance between a least-squares fit curve and its data is due more to data scatter than the lack-of-fit of the regression line so it is more likely that the regression line is, indeed, a good fit to the data. Q is presented in the last column of the table and the percentage confidence that the

Table 2. Statistical evaluation of differences between frequency distributions as functions of d in static sperm suspensions

Data from	Regression curve from	d.f.	Q <
t = 0 min	t = 0	9, 26	0·025
t = 30 min	t = 0	10, 28	0·001
t = 45 min	t = 0	11, 30	0·001
t = 60 min	t = 0	8, 24	0·050
t = 30 min	t = 30	10, 28	0·001
t = 45 min	t = 45	11, 30	0·005
t = 60 min	t = 60	8, 24	0·050

curve fits the data is (1·000 − Q) × 100. The relatively 'poor' fits of the t = 0 ((1·000 − 0·025) × 100 = 97·5%) and t = 60 (95%) curves to their own data and each other (95%) are still quite good.

The STAT curves in general appear to show no particular progression from t = 0 to t = 60. In each case the incidence of motile spermatozoa falls to essentially zero at about 100 μm from the wall, leaving the centre third of the tube vacated. Another persistent pattern is the drop in f at the wall. While the error bars at d = 0 and d = 10 μm do overlap, the f averages in all four plots are lower at d = 0.

In the two flow systems the same general lack of variation in motile sperm frequency distribution with time persists, as shown in Text-fig. 8. While f drops to zero in some cases by d =

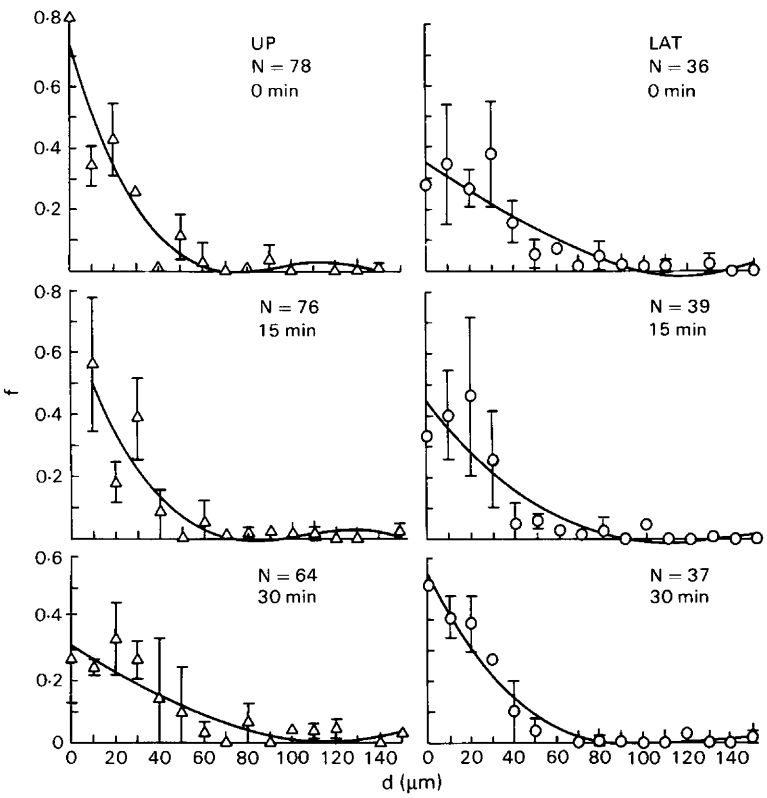

Text-fig. 8. Frequency distribution of spermatozoa as a function of d for different times after pumping of the first spermatozoa of a sample into the chamber where the fluid is flowing upwards or laterally. N = total number of frequencies used.

70 μm (e.g. at $t = 0$ in UP) the curves are similar to those of the static system. Indeed, the F statistic analysis which is summarized in Table 3 shows that the deviation from the STAT plots suggested by the curves for UP at $t = 0$ and $t = 15$ does not fit the data from UP at $t = 30$. This effect is almost certainly due to the lower f values at d = 0 and d = 10 μm in the latest measurement. The last two rows in the table evaluate the fit of UP and LAT data at $t = 30$ to the regression curve from STAT at $t = 30$. The regression curve from the latter, in contrast, matches the STAT data at $t = 30$ at the $Q < 0{\cdot}001$ level. The regression curve for f at $t = 0$ in the lateral flow systems fits all times for this orientation to at least the 99·5% confidence level. Moreover, the match of the STAT curve to the LAT data at $t = 30$ reaches the 99·9% confidence level.

Table 3. Statistical evaluation of differences between frequency distributions as functions of d in flowing sperm suspensions

Flow direction	Data from	Regression curve from	d.f.	Q <
UP	$t = 0$ min	$t = 0$ min	10, 28	0·001
UP	$t = 15$ min	$t = 0$ min	10, 28	0·001
UP	$t = 30$ min	$t = 0$ min	11, 30	No fit
LAT	$t = 0$ min	$t = 0$ min	11, 30	0·001
LAT	$t = 15$ min	$t = 0$ min	12, 32	0·005
LAT	$t = 30$ min	$t = 0$ min	11, 30	0·005
UP	$t = 30$ min	$t = 30$ min	11, 30	0·005
LAT	$t = 30$ min	$t = 30$ min	11, 30	0·001
UP	$t = 30$ min	STAT $t = 30$ min	11, 30	0·001
LAT	$t = 30$ min	STAT $t = 30$ min	11, 30	0·001

Unlike the pattern in the static systems, there is no consistent tendency for a drop in f at the wall for these flow system data. Notwithstanding these results which represent a mixture of frequencies (some specimens had no readings at d = 0, some had readings at d = 50 and d = 90 while others were read only at d = 60, etc.), the drop in f at the wall shows up dramatically in the larger flow system populations represented in Text-fig. 6. Indeed, there is very little overlap in error bars between the d = 0 and d = 10 μm f values in either lateral or upward flow. One must be cautious in comparing Text-figs 6 with 8 because the f at d = 0 is an average of more than one semen sample in the former while the high f values for d = 0 at $t = 0$ in Text-fig. 8 are from one sample.

Conclusions

The dominating characteristic of sperm distribution in a tube is their tendency to accumulate near the walls. The frequency distribution that appears as soon as the cells can be pumped into the observation tube does not change significantly over a 1-h period whether the fluid is flowing or static. The form of the distribution is probably best characterized by the regression curves of Text-fig. 6 with the exception of their concentration near the wall. At the wall the number of motile spermatozoa swimming at $V \geq 30$ μm/sec is at least 30% less than at 10 μm from the wall. Obviously, these swimmers are not stuck on the wall so the boundary effect is not an electrostatic artefact. From the d = 10 μm position where about one third of the spermatozoa accumulate to d = 100 μm the frequency drops gradually to zero. Therefore, in tubes < 200 μm wide we would expect an inverse relationship between calibre and frequency of spermatozoa in the tube centre.

The second most important contributor to sperm distribution is negative rheotaxis which appears where the shear rate (velocity gradient) is around 3·5 sec^{-1}, a value which is in good agreement with the 3 sec^{-1} optimum value for negative rheotaxis obtained for bull spermatozoa by Roberts (1970). Negative rheotaxis is easily accounted for by the accumulation tendency. As cells

swim from the tube centre towards the walls their heads are in a layer of the flow profile which is moving slower than the layer surrounding their tails. As a result the tails are rotated downstream relative to the heads. The report of Kono *et al.* (1977) of no negative rheotaxis for rabbit and cock spermatozoa in 3 mm and 300 μm tubes may be explained by their maximum u(d) of 100 μm/sec which could not develop the minimum shear rate required for this behaviour (100 μm sec^{-1}/150 μm gives an average shear rate of 0·667 sec^{-1}). The tendency for cos θ to be markedly positive at the wall (see Text-figs 3 & 4) is difficult to explain as a rheotaxis. No such skew was found in the static systems (at the wall $G_r = 0{\cdot}926$). The tube system was open ended so no back flow (which would tend to be at the tube axis in any case) was present. No fluid rotation suggesting secondary flows was ever observed. Development of a significant zeta potential between the moving suspension and no-slip fluid at the wall seems far-fetched. The published models for rheotaxis would predict our observations if the cells were swimming away from the wall (Roberts, 1970), a result made unlikely by their tendency to accumulate within one body length (head + tail) of the wall. Consequently, the interpretation of this result will have to await a more extended analysis of individual swimming paths.

The relative influence of the velocity gradient on sperm orientation is suggested by its overwhelming of any geotaxic effect in a flowing system. This conclusion arises directly from the insignificant difference between rheotaxis in lateral flowing and upward flowing suspensions. One should not be surprised by the relative insignificance of the geotaxic effect. If Stokes' law for a sedimenting body is applied to the head of a spermatozoon assuming a net radius of 1·15 μm and specific gravity of 1·30 (from Katz & Pedrotti, 1977), a sedimentation velocity of 0·86 μm/sec is obtained. The slowest spermatozoon we measured swam more than 34 times this velocity and not necessarily in a straight line.

The strength of rheotaxis relative to thigmotaxis, in contrast, is small. The inability of flow to cause any significant change in the frequency distribution pattern between static and flowing suspension leads us to the conclusion that the 'inelastic collision' effect (Rothschild, 1963), or as we prefer 'boundary effect', dominates rheotaxis.

In static suspensions geotaxis and the boundary effect interact alone but the gravitational effect is so comparatively weak that the vertical distribution of spermatozoa is of interest only when the closest opposing boundaries are horizontal as was the case in Rothschild's (1963) study. Accordingly, when spermatozoa are being studied in a system in which they are required to swim from some point near the upper surface of the suspension, 11 will swim downwards for each 9 that swim upwards. And if the fluid column is long enough nearly all of them will end up within 100 μm of the side walls.

Discussion

Given the above conclusions we can make some predictions about sperm behaviour *in vivo* and *in vitro* in terms of their responses to mechanical stimuli.

In-vitro considerations include laboratory techniques which depend upon vertical swimming to select spermatozoa. One can produce higher yields in the bottom layers if the cells are collected near the side walls adjacent to the bottom of the container as well as at the very bottom boundary. If the container is wider than tall the percentage at the bottom will be greatest. If it is taller than wide the percentage at the side boundaries will be greatest. Techniques such as that of Ericsson *et al.* (1973), which add a vertical viscosity gradient to the mechanical environment, separate X- and Y-bearing spermatozoa by amplifying the difference in swimming velocity (Goodall & Roberts, 1976). The Y-bearing spermatozoa in any one albumin layer would not only reach the bottom of the layer but also the side walls much faster than would the X-chromosome bearers.

When suspension flow is added to a system for which sperm selection is the goal, any prediction must take into account the effect of negative rheotaxis on net distribution of fast (Y) and slow (X)

swimmers. At the distances from the container wall where the shear rate is 3–4 sec^{-1} one should be able to collect a percentage of faster swimmers (presumably Y spermatozoa) which increases with time and upstream distance. The slower swimmers (presumably X spermatozoa) and non-reorientating cells would be carried towards the downstream end of the tube. Thus, one could theoretically separate X and Y spermatozoa in the system used in the present study and periodically collect samples (a constant sampling device would distort the flow pattern) rich in the latter from the region $40 \leq d \leq 60$ μm near the upstream end of the tube. The X spermatozoa would be in higher concentration at the same d region at the downstream end of the tube but the sample would be contaminated with poorer swimmers bearing X or Y chromosomes.

The tendency for spermatozoa to concentrate near but not on the wall (see Text-fig. 6) would aid any collection procedure as cells on the wall would more easily resist being sucked up because they would have some protection from the 'no-slip' fluid boundary layer next to the wall.

These interactions of rheotaxis with boundary effects are contributing factors to the success of the system used by Bhattacharya *et al.* (1977) for separating X and Y spermatozoa. Since no dimensions or flow values or directions are specified in their report we cannot quantitatively compare our measurements with their "before galvanization" results.

The success of the Atherton (1975) technique for motility assessment is explained by our results, particularly those presented in Text-figs 3 & 4. During the flow phase of Atherton's (1975) procedure enough negative rheotaxis occurs to align spermatozoa concentrated near the wall by the boundary effect. When flow stops they resume random motion in the near-wall optical plane which is perpendicular to the spectrophotometer beam. Therefore, because there are few motile spermatozoa at the tube centre line, it is those concentrated near the vertical walls through which the beam passes and generates the desired measurements. Further, the technique would be optimized by keeping the beam as far as possible from the points at which the tube axis curves because fluids moving around curves often develop secondary flows which would carry spermatozoa near the wall towards the tube axis.

In vivo, suspensions of motile spermatozoa encounter three major mechanical reproductive vessel environments: (1) tubes such as the vas deferens and uterus in which wall calibre changes with time at any position along the tube axis due to contraction of circular smooth muscle; (2) tubes such as the uterotubal junction which are lined with flow-generating cilia; and (3) non-Newtonian fluids in tubes such as the cervical canal and ampulla in which spermatozoa must penetrate 'boundaries' of high viscosity (e.g. mucus or cumulus oophorus). The evidence for the importance of the boundary effect helps us make some predictions about the influence of boundaries on sperm transport and transit *in vivo*. For example, any significant periodic constriction of tubes carrying motile spermatozoa creates secondary flows which counteract the boundary effect by carrying the cells towards the tube axis. Moreover, since the majority of spermatozoa do not accumulate on the wall, few swimmers can avoid secondary flow mixing by hiding in a boundary layer. In this manner contracting tubes will reverse the radial concentration tendency of spermatozoa if they can generate sufficient secondary flow. Unfortunately, so little is known of the contraction patterns along the female tract that there is insufficient basis for any quantitative prediction of where spermatozoa will tend to be in a given tube segment. We would, however, guess that uterine and isthmic contractions as described by Verdugo, Lee, Halbert, Blandau & Tam (1980) are sufficient to disrupt the boundary effect significantly.

Ciliated epithelium provides a boundary which is itself generating steady flow in a tube. The boundary effect described in the present report must be refined to allow for the added influence of an array of oscillating filaments. Secondary flows due to local ciliary effects are far smaller than those due to tubal contractions. Nevertheless, currents generated by these co-ordinated oscillators may be too strong and ciliary packing too dense for spermatozoa to accumulate near the wall. Observations (unpublished) of preparations of human spermatozoa swimming over a field of frog ciliated epithelium revealed that the swimming spermatozoa could not penetrate to within 50 μm of the active cilia.

Another factor to consider in analysing sperm behaviour in flows generated by ciliated tubes is the tendency for pressures to build up downstream which generate backflow in the tube centre. Accordingly, in the isthmus where cilia beat towards the uterus (Blandau & Verdugo, 1976), backflow must occur due to the build-up of pressure at the uterotubal junction (Blake, Vann & Winet, 1983). After consideration of all these factors we can predict that cilia in the isthmus tend to generate axial flow towards the ampulla and counteract the tendency for spermatozoa to concentrate near the tube wall. As a result spermatozoa will tend to accumulate near the isthmic tube centre and be swept toward the ampulla.

What role does rheotaxis play in this isthmus scenario? We have reported shear rates up to 25 sec^{-1} (Winet, Yates, Wu & Head, 1984) near ciliary tips and the presence of backflow in a ciliated tube would allow values of 3–4 sec^{-1} to persist at relatively large distances from the wall. One cannot yet specify these d values because there are no reported measurements of backflow in a tube such as the isthmus or of the pressures associated with such backflow. We can, nevertheless, predict that the basic boundary effect would result in a tendency for negatively rheotaxic spermatozoa to swim towards the uterus.

From the foregoing it is clear that the interactions of currents near ciliated epithelium, the boundary effect, backflow and rheotaxis are too complex to allow simple predictions of the location of a given spermatozoon of known motility in the isthmus. When muscular contractions are added to the environment, one can appreciate the difficulty of developing a useful model for sperm travel through the isthmus.

Boundaries composed of non-Newtonian fluids such as cervical mucus or cumulus oophorus do not present wall-motion analysis problems as they do not generate fluid flows. They do, nonetheless, force us again to refine our concept of a boundary because non-Newtonian fluids by definition change their viscosity in response to shear and, in these two media, proteinases which may be secreted by the spermatozoa. The unique feature of this system is that a boundary may be converted to part of the swimming medium and *vice versa*. Hence the boundary effect now becomes a function of swimming behaviour. The upshot of these interactions is a local mechanical feedback system of changing boundary effect and swimming orientation. Rheotaxis plays no significant role in this behaviour due to the absence of flow in the pure system. But the solation of the non-Newtonian matrix and the ability of the remaining matrix to reorientate the spermatozoa mechanically (Tampion & Gibbons, 1962) has the rheotaxis-like effect of aligning individuals parallel with one another (see Gaddum-Rosse, Blandau & Lee, 1980).

There are numerous models for the behaviour of spermatozoa in non-Newtonian fluids such as cervical mucus (see Katz & Berger, 1980) so we shall not explore their details. It is, however, clear that the basic boundary effect described herein is replaced by a local boundary effect in mucus (or cumulus) which keeps the spermatozoa from turning towards and accumulating near the walls of the vessel, although they can reach the walls of the cervix by following the strain lines in the mucus created by the secretion process.

All three of the environmental factors we have considered may co-exist or take effect sequentially in a number of reproductive tubes such as the cervix, uterotubal junction and ampulla. The difficulties cited for predicting specific sperm distributions in response to any one factor would, of course, be compounded in a combination system.

Finally we must emphasize our original use of quotes for the terms 'geotaxis', 'rheotaxis' and 'thigmotaxis' which were dropped in the remaining text for convenience. There is no evidence from the present results to deny the statement (see 'Introduction') that spermatozoa show no ability to transduce physiologically mechanical input from their environment. Accordingly, none of the behaviour described herein should be considered as 'taxes' in the traditional sense.

Financial support was provided by National Institutes of Health grants HD12101 and HD15442 from the National Institute of Child Health and Human Development to H.W.

References

Adolphi, H. (1905) Die Spermatozoen der Saugetiere schwimmen gegen den Strom. *Anat. Anz.* **26**, 549–559.

Atherton, R.W. (1975) An objective method for evaluating Angus and Hereford sperm motility. *Int. J. Fert.* **20**, 109–112.

Bhattacharya, B.C., Shome, P. & Gunther, A.H. (1977) Successful separation of X and Y spermatozoa in human and bull semen. *Int. J. Fert.* **22**, 30–35.

Blake, J.R., Vann, G. & Winet, H. (1983) A model of ovum transport. *J. theor. Biol.* **102**, 145–166.

Blandau, R.J. & Verdugo, P. (1976) An overview of gamete transport; comparative aspects. *In Ovum Transport and Fertility Regulation*, pp. 138–146. WHO, Geneva.

Bretherton, F.P. & Rothschild, L. (1961) Rheotaxis of spermatozoa. *Proc. R. Soc. B* **153**, 490–502.

Ericsson, R.J., Langevin, C.N. & Nishino, M. (1973) Isolation of fractions rich in human Y sperm. *Nature, Lond.* **246**, 421–424.

Gaddum-Rosse, P., Blandau, R.J. & Lee, W.I. (1980) Sperm penetration into cervical mucus *in vitro*. I. Comparative studies. *Fert. Steril.* **33**, 636–643.

Goodall, H. & Roberts, A.M. (1976) Differences in motility of human X- and Y-bearing spermatozoa. *J. Reprod. Fert.* **48**, 433–436.

Katz, D.F. & Berger, S.A. (1980) Flagellar propulsion of human sperm in cervical mucus. *Biorheology* **17**, 169–175.

Katz, D.F. & Pedrotti, L. (1977) Geotaxis by motile spermatozoa: hydrodynamic reorientation. *J. theor. Biol.* **67**, 723–732.

Kono, K., Morohashi, K., Kinose, Y., Hiura, Y. & Yamamoto, K. (1977) Rheotaxis of spermatozoa in domestic animals. II. Orientation of rabbit and cock spermatozoa in the flow of fluid in fine tubes. *Japan J. Anim. Reprod.* **23**, 47–54.

Pollard, J.H. (1977) *A Handbook of Numerical and Statistical Techniques*, pp. 255–299. Cambridge University Press.

Roberts, A.M. (1970) Motion of spermatozoa in fluid streams. *Nature, Lond.* **228**, 375–376.

Roberts, A.M. (1972) Gravitational separation of X and Y spermatozoa. *Nature, Lond.* **238**, 223–225.

Rothschild, L. (1963) Non-random distribution of bull spermatozoa in a drop of sperm suspension. *Nature, Lond.* **198**, 1221–1222.

Sarkar, S. (1981) Human X and Y sperm: a laminar flow method of *in vitro* separation. *Fedn Proc. Fedn Am. Socs exp. Biol.* **40**, 763.

Tampion, D. & Gibbons, R.A. (1962) Orientation of spermatozoa in mucus of the cervix uteri. *Nature, Lond.* **194**, 381–382.

Verdugo, P., Lee, W.I., Halbert, S.A., Blandau, R.J. & Tam, P.Y. (1980) A stochastic model for oviductal egg transport. *Biophys. J.* **29**, 257–270.

Walton, A. (1952) Flow orientation as a possible explanation of 'wave motion' and 'rheotaxis' of spermatozoa. *J. exp. Biol.* **29**, 520–531.

Winet, H. & Head, J. (1982) Direction of spermatozoon swimming in response to gravity, fluid flow and solid walls. *J. Androl.* **3**, 27, Abstr.

Winet, H., Yates, G.T., Wu, T.Y. & Head, J. (1984) On the mechanics of mucociliary flows. III. Flow velocity profiles in frog palate mucus. *J. appl. Physiol.* (in press).

Received 7 July 1983